

Warsaw Breakage Syndrome DDX11 helicase acts jointly with RAD17 in the repair of bulky lesions and replication through abasic sites

Takuya Abe^{1,2,#}, Masato Ooka^{1,2,#}, Ryotaro Kawasumi¹, Keiji Miyata², Minoru Takata³, Kouji Hirota², and Dana Branzei^{1,4,*}

Supplementary Information

1 Table

Methods

References

6 Figures

Table S1. Cell lines used in the study

Genotype	Selective marker	Reference	Strain No.	
WT	-	(55)	8	
<i>DDX11</i> ^{-/-}	<i>DDX11/DDX11::</i> KO-Puro/KO-Bsr	(27)	122	
<i>DDX11</i> ^{-/-} + <i>hDDX11</i>	<i>DDX11/DDX11::</i> KO-Puro/KO-Bsr, + <i>DDX11::</i> Neo	This study	129	130
<i>DDX11</i> ^{-/-} + ^{GFP} <i>cDDX11</i> ^{HA}	<i>DDX11/DDX11::</i> KO-Puro/KO-Bsr, + <i>GFP-cDDX11-HA::</i> Neo	(27)	131	132
<i>DDX11</i> ^{-/-} + ^{GFP} <i>cDDX11-K87A</i> ^{HA}	<i>DDX11/DDX11::</i> KO-Puro/KO-Bsr, + <i>GFP-cDDX11-K87A-HA::</i> Neo	(27)	177	178
<i>FANCC</i> ^{-/-}	<i>FANCC::</i> KO-Bsr	(56)	9	
<i>DDX11</i> ^{-/-} <i>FANCC</i> ^{-/-}	<i>DDX11/DDX11::</i> KO-Puro/KO-Bsr, <i>FANCC::</i> KO-His	This study	136	137
<i>FANCI</i> ^{-/-}	<i>FANCI/FANCI::</i> KO-Bsr/KO-His	(57)	10	
<i>DDX11</i> ^{-/-} <i>FANCI</i> ^{-/-}	<i>DDX11/DDX11::</i> KO-Puro/KO-Bsr, <i>FANCI/FANCI::</i> KO-His/KO-Eco	This study	146	147
<i>RAD18</i> ^{-/-}	<i>RAD18/RAD18::</i> KO-His/KO-Hyg	(58)	193	
<i>RAD18</i> ^{-/-} <i>DDX11</i> ^{-/-}	<i>RAD18/RAD18::</i> KO-His/KO-Hyg, <i>DDX11/DDX11::</i> KO-Puro/KO-Bsr	This study	211	212
<i>BRCA2</i> ^{-/-} <i>DDX11</i> ^{-/-} + <i>MerCreMer</i>	<i>BRCA2/BRCA2::</i> KO- Bsr(removed)/KO-Puro(removed), <i>DDX11/DDX11::</i> KO-Bleo/KO-His, + <i>MerCreMer::</i> Neo	This study	219	220
<i>BRCA2</i> ^{-/-} + <i>MerCreMer</i>	<i>BRCA2/BRCA2::</i> KO- Bsr(removed)/KO-Puro(removed), + <i>MerCreMer::</i> Neo	(59)	201	202
<i>RAD17</i> ^{-/-}	<i>RAD17::</i> KO-His	(60)	366	
<i>DDX11</i> ^{-/-} <i>RAD17</i> ^{-/-}	<i>DDX11/DDX11::</i> KO-Puro/KO-Bsr, <i>RAD17::</i> KO-His	This study	369	374
<i>PRIMPOL</i> ^{-/-}	<i>PRIMPOL/PRIMPOL::</i> KO-Bsr/KO- Puro	(61)	R147	
<i>DDX11</i> ^{-/-} <i>PRIMPOL</i> ^{-/-}	<i>PRIMPOL/PRIMPOL::</i> KO-Bsr/KO- Puro, <i>DDX11/DDX11::</i> KO-His/KO- Hyg	This study	M001	M002
WT + <i>DR-GFP</i> + <i>teton-I-SceI</i>	+ <i>DR-GFP::</i> Puro, + <i>tet3G +I- SceI::</i> Neo	(34)	105	106
<i>DDX11</i> ^{-/-} + <i>DR- GFP</i> + <i>tet3G +I- SceI</i>	<i>DDX11/DDX11::</i> KO-Bleo/KO-His, + <i>DR-GFP::</i> Puro, + <i>tet3G +I- SceI::</i> Neo	This study	111	112
WT + <i>DR-GFP</i> + <i>tet3G +I- SceI</i> + <i>tet3G-BRC4</i>	+ <i>DR-GFP::</i> Puro, + <i>tet3G +I- SceI::</i> Neo, + <i>BRC4::</i> Bsr	(34)	322	323
WT + <i>tet3G- hSA2</i> ^{9xMyc}	+ <i>tet3G::</i> Neo, + <i>hSA2-9xMyc::</i> His	(27)	246	279
WT + <i>tet3G- hSA2-12A</i> ^{9xMyc}	+ <i>tet3G::</i> Neo, + <i>hSA2-12A- 9xMyc::</i> His	(27)	228	283

<i>DDX11</i> ^{-/-} + <i>tet</i> - <i>hSA2</i> ^{9xMyc}	<i>DDX11/DDX11::KO</i> -Puro/ <i>KO</i> -Bsr, + <i>tet</i> 3G:: <i>Neo</i> , + <i>hSA2-9xMyc::His</i>	(27)	227	281
<i>DDX11</i> ^{-/-} + <i>tet</i> - <i>hSA2-12A</i> ^{9xMyc}	<i>DDX11/DDX11::KO</i> -Puro/ <i>KO</i> -Bsr, + <i>tet</i> 3G:: <i>Neo</i> , + <i>hSA2-12A-9xMyc::His</i>	(27)	230	285
<i>RAD17</i> ^{-/-} + <i>tet</i> - <i>hSA2</i> ^{9xMyc}	<i>RAD17::KO</i> -Hyg, + <i>tet</i> 3G:: <i>Neo</i> , + <i>hSA2-9xMyc::His</i>	This study	M40	
<i>RAD17</i> ^{-/-} + <i>tet</i> - <i>hSA2-12A</i> ^{9xMyc}	<i>RAD17::KO</i> -Hyg, + <i>tet</i> 3G:: <i>Neo</i> , + <i>hSA2-12A-9xMyc::His</i>	This study	M42	

Supplementary Methods

Plasmid DNA and cell lines

The list of cell lines used in this study is described in the Key Resources Table. Knock-out constructs and cell lines for *DDX11* (1), *BRCA2* (2), *RAD18* (3), *RAD17* (4), *FANCC* (5), *FANCI* (6), *Primpol* (7) have been previously described.

Assessment of Cell Growth and Sensitivity to DNA damaging Agents

Cells were cultured at 39.5°C in D-MEM/F-12 medium (Gibco) supplemented with 10% fetal bovine serum, 2% chicken serum (Sigma), Penicillin/Streptomycin mix, and 10 µM 2-mercaptoethanol (Gibco). To plot growth curves, each cell line was cultured in three different wells of 24 well-plates and passaged every 24 h. The cell number was determined by flow cytometry using plastic microbeads (07313-5; Polysciences). Cell solutions were mixed with the plastic microbead suspension at a ratio of 10:1, and viable cells, determined by forward scatter and side scatter, were counted when a given number of microbeads was detected by flow cytometry. To assess drug sensitivity, 1 x 10⁴ cells were cultured in 24-well plates containing various concentrations of DNA-damaging agents in 1 ml of medium in duplicate. Cell viability was assessed after 48 h

by flow cytometry using plastic microbeads. Percent survival was determined by considering the number of untreated cells as 100%. To determine CDDP and MMS sensitivity by Colony survival assay, 4×10^2 cells were inoculated into 60-mm dishes containing various concentrations of drug in a medium supplemented with 1.5% (wt/vol) methylcellulose, 15% fetal bovine serum, and 1.5% chicken serum. Colonies were counted after 7–14 days, and the percent survival was determined relative to the number of colonies of untreated cells.

DNA Transfection and RT-PCR

DNA transfection and RT-PCR were performed as described previously (8). Drug-resistant colonies were selected in 96-well plates in medium containing 0.5 $\mu\text{g/ml}$ puromycin, 30 $\mu\text{g/ml}$ blasticidin, 1 mg/ml L-histidinol, 10 $\mu\text{g/ml}$ mycophenolic acid, 2 mg/ml geneticin, 1 mg/mL bleomycin, or 2.5 mg/ml hygromycin B, as appropriate. Gene disruption was verified by genomic PCR and RT-PCR. The primers used for RT-PCR are available upon request.

DR-GFP assay

The DR-GFP construct containing two mutant GFP and I-SceI site was integrated at OVA region on chromosome 2. The I-SceI enzyme was expressed by Tet-On 3G system and DSBs were induced. The percentage of GFP expressing recombinant cells was measured by FACS as previously shown (8).

Detection of chromosome aberrations and sister chromatid exchanges

To analyze chromosome aberrations, cells were cultured in the presence of 10 or 20 ng/ml MMC for 16 h and then treated with colcemid for the last 135 min. Cells were

harvested, treated with 75 mM KCl for 15 min, and then fixed with methanol-acetic acid (3:1) for 30 min. The cell suspension was dropped onto wet cold glass slides, air-dried, and stained with 3% Giemsa solution at pH 6.8 for 20 min and examined with a light microscope. To measure sister chromatid exchanges (SCEs), cells were cultured for two cycle periods in medium containing 10 μ M BrdU and then treated with colcemid for the last 135 min. Cells were harvested and fixed as described above. To induce DNA damage, cells were treated with 100 nM CDDP for 16.5 h just before harvesting.

Cell Cycle Analysis by Flow Cytometry

To assess cell cycle progression, cells were harvested, fixed in 70% ethanol, stained with propidium iodide (PI), and analyzed by flow cytometry as previously shown with some small modifications (9). For two-dimensional cell cycle analysis, cells were cultured in medium containing 20 μ M bromodeoxyuridine (BrdU; BD Biosciences) for 20 min just before harvesting. Cells were fixed in 70% ethanol, treated with 2.5 M HCl, and incubated with anti-BrdU antibody (BD Biosciences). The BrdU antibody was stained with FITC-conjugated goat Anti-Mouse IgG H&L antibody (Sigma). Cells were also stained with 1 μ g/ml PI and RNA was removed by RNase treatment. Cell cycle distribution was analyzed by flow cytometry.

DNA Fiber Assay

DNA fiber assay was performed as previously shown with some small modifications (9). Cells (5×10^5 in 1 mL of medium) were pulse-labeled with 25 μ M chlorodeoxyuridine (CldU; Sigma) and then sequentially pulse-labeled with 250 μ M iododeoxyuridine (IdU; Sigma). Cells were resuspended in ice-cold PBS and then dropped onto glass slides

(PRESTIGE). Cells were lysed with DNA fiber lysis buffer (0.5% SDS, 200 mM Tris-HCl, pH 7.4, 50 mM EDTA), and then glass slides were tilted to extend DNA. For fixation, glass slides were immersed in Carnoy fluid (MeOH:AcOH, 3:1) for 3 min, then 70% EtOH for 1 h to overnight. After washing with PBS, glass slides were immersed in 2.5 M HCl for 30 min to denature DNA molecules and subsequently in 0.1 M sodium tetraborate for 3 min to neutralize the acid. After washing with PBS, the slides were treated with rat anti-BrdU antibody (1:200; Abcam) and mouse anti-BrdU antibody (1:50; BD Biosciences), which reacted against CldU and IdU, respectively. Cy3-conjugated anti-rat IgG (1:400; Jackson ImmunoResearch) and Alexa Fluor 488 anti-mouse IgG (1:100; Invitrogen) were used as the secondary antibodies. The first and second antibodies were incubated for 1 h at room temperature, respectively. Washing of antibodies was performed with 0.05% Tween 20 in PBS. Coverslips were mounted with Shandon* PermaFluor (Invitrogen). Images were captured with a fluorescence microscope. Fiber lengths were measured using ImageJ, and micrometer values were expressed in kilobases using the following conversion factor: 1 μm = 2.59 kb. Measurements were recorded from areas of the slides with untangled DNA fibers to prevent the possibility of recording labeled patches from tangled bundles of fibers.

Visualization of RAD51 and γ H2AX subnuclear foci

After MMC exposure (500 ng/mL, 1h), cells were harvested and spun onto glass slides using Cytospin. Cells were pre-permeabilized with 0.1% (v/v) Triton X-100 in PBS, fixed with 4% paraformaldehyde and permeabilized with 0.5% (v/v) Triton X-100 in PBS. Slides were then incubated with anti-Rad51 antibodies (Santacruz; sc-8349) and anti- γ H2AX antibodies (Millipore; 05-636). Alexa-Fluor 488 goat anti-rabbit IgG (Invitrogen) and Cy3- conjugated donkey anti-mouse IgG (Jackson ImmunoResearch)

were used as secondary antibody and 0.1 $\mu\text{g}/\text{mL}$ DAPI was used for counterstaining. We only scored RAD51- and γH2AX -foci positive and negative cells with non-apoptotic nuclei. Images were captured with a fluorescent microscope (BX51, OLYMPUS).

Western Blotting

Western blotting was carried out as described previously (9). Cells were suspended in SDS sample buffer (50 mM Tris-HCl, pH 6.8, 0.1 M DTT, 2% SDS, 10% glycerol, 0.1% bromphenol blue). The primary antibodies used were anti-phospho-Check1 (Chk1)-Ser345 (2341, Cell Signaling Technology), PCNA (PC-10, Santa Cruz), anti-Histone H3 (ab1791, Abcam), and anti-FANCD2 (10). Horseradish peroxidase-conjugated anti-rabbit IgG (Cell Signaling Technology) was used as a secondary antibody. Proteins were visualized using SuperSignal West Femto Western blotting detection reagents (Thermo Fisher Scientific). Images were captured with ChemiDoc XRS Plus (Biorad).

AID overexpression by retrovirus infection

AID overexpression was carried out as described previously (11). Several single colonies were obtained from WT and each mutant. The cells which are overexpressing AID were cultured for 2 weeks. AID overexpression was carried out by infection of retrovirus containing the AID gene and the internal ribosomal entry site (IRES) followed by the Green fluorescent protein (GFP) gene. The efficiency of infection was about 60%, as measured by GFP expression.

sIgM gene conversion assay

The Ig gene conversion assay was carried out as described previously (12). DT40 has a frameshift in its rearranged V segment, which can be repaired by homologous

pseudogene sequences. IgM negative cells from each genotype were cultured for 2 weeks. After collecting the cells, cells were treated with FITC-conjugated α -IgM antibody (BETHYL) and washed by SB (PBS containing 1% BSA). After that, cells were resuspended in SB. Cells were analyzed for sIgM expression by fluorescence-activated cell sorting (FACSCalibur, BD biosciences).

Analysis of IgV λ diversification

Genomic DNA was extracted at 14 days post infection. Using primers CVLF6 5'-CAGGAGCTCGCGGGGCCGTCACTGATTGCCG and CVLR3 5'-GCGCAAGCTTCCCCAGCCTGCCGCAAGTCCAAG, the rearranged V segments were PCR amplified, with Prime Star GXL DNA polymerase (Takarabio, Shiga, Japan), a high fidelity thermostable polymerase, cloned into pTOPO II -ZeroBlunt (Invitrogen) and sequenced with the M13 forward (-21) primer. Sequence alignment with clustalW (GenomeNet, Kyoto, Japan; <https://www.genome.jp/>) allowed identification of changes from the parental sequences in each clone. After the alignment, mutations were classified into Gene Conversion (GC) or Hypermutation (PM) as described previously (13).

Supplementary References

1. Abe T, *et al.* (2016) Chromatin determinants of the inner-centromere rely on replication factors with functions that impart cohesion. *Oncotarget* 7(42):67934-67947.
2. Qing Y, *et al.* (2011) The epistatic relationship between BRCA2 and the other RAD51 mediators in homologous recombination. *PLoS Genet* 7(7):e1002148.

3. Yamashita YM, *et al.* (2002) RAD18 and RAD54 cooperatively contribute to maintenance of genomic stability in vertebrate cells. *EMBO J* 21(20):5558-5566.
4. Kobayashi M, *et al.* (2004) Critical role for chicken Rad17 and Rad9 in the cellular response to DNA damage and stalled DNA replication. *Genes Cells* 9(4):291-303.
5. Hirano S, *et al.* (2005) Functional relationships of FANCC to homologous recombination, translesion synthesis, and BLM. *EMBO J* 24(2):418-427.
6. Wu Y, *et al.* (2010) Fanconi anemia group J mutation abolishes its DNA repair function by uncoupling DNA translocation from helicase activity or disruption of protein-DNA complexes. *Blood* 116(19):3780-3791.
7. Kobayashi K, *et al.* (2016) Repriming by PrimPol is critical for DNA replication restart downstream of lesions and chain-terminating nucleosides. *Cell Cycle* 15(15):1997-2008.
8. Abe T & Branzei D (2014) High levels of BRC4 induced by a Tet-On 3G system suppress DNA repair and impair cell proliferation in vertebrate cells. *DNA Repair* 22:153-164.
9. Hosono Y, *et al.* (2014) Tipin functions in the protection against topoisomerase I inhibitor. *J Biol Chem* 289(16):11374-11384.
10. Shigechi T, *et al.* (2012) ATR-ATRIP kinase complex triggers activation of the Fanconi anemia DNA repair pathway. *Cancer Res* 72(5):1149-1156.
11. Hirota K, *et al.* (2015) The POLD3 subunit of DNA polymerase delta can promote translesion synthesis independently of DNA polymerase zeta. *Nucleic Acids Res* 43(3):1671-1683.

12. Arakawa H, Hauschild J, & Buerstedde JM (2002) Requirement of the activation-induced deaminase (AID) gene for immunoglobulin gene conversion. *Science* 295(5558):1301-1306.
13. Sale JE, Calandrini DM, Takata M, Takeda S, & Neuberger MS (2001) Ablation of XRCC2/3 transforms immunoglobulin V gene conversion into somatic hypermutation. *Nature* 412(6850):921-926.

Supplementary Figures

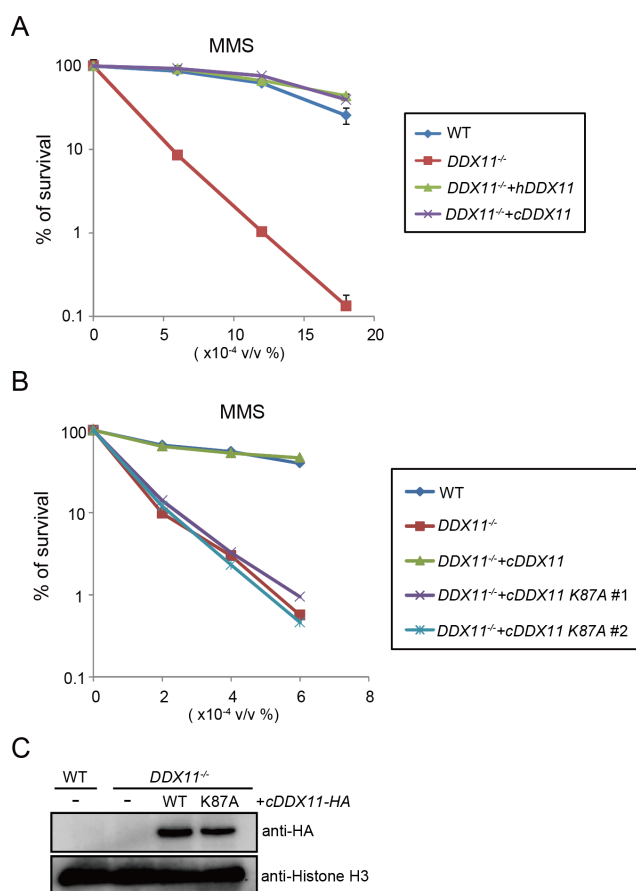


Figure S1. DDX11 helicase facilitates ICL repair.

(A-B) Sensitivity of cells of the indicated genotypes to chronic MMS treatment. Colony/Cell survival percentage is displayed as the ratio of the number of surviving colonies (A) or cells (B) following the indicated treatment relative to the untreated control. Each line and error bar represents the mean value and SD from two independent experiments, respectively. (C) Western blot to check the expressed levels of WT and helicase dead (K87A) cDDX11-HA levels. Fig. S1 relates to Fig. 1.

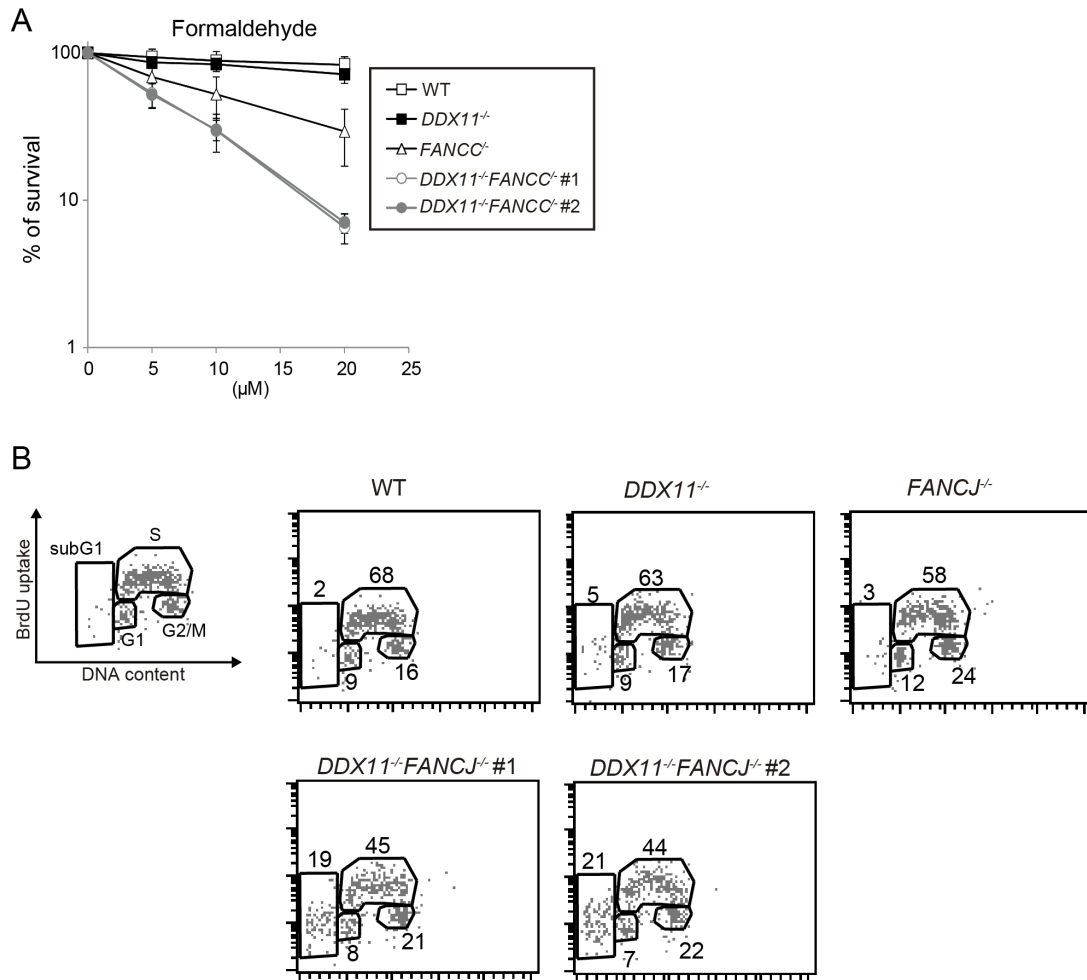


Figure S2. Synthetic interactions between *ddx11* and *fance/fancj* mutants. (A) Sensitivity of cells of the indicated genotype to Formaldehyde as in Fig. 1B. (B) Cell cycle distribution of WT, *DDX11*^{-/-}, *FANCC*^{-/-} and *DDX11*^{-/-} *FANCC*^{-/-} cells. Cells were pulse-labeled with BrdU for 15 min, and harvested. The cells were incubated with anti-BrdU antibody to detect BrdU uptake, which was further stained with FITC-conjugated anti-mouse IgG antibody. PI was used to detect DNA. The vertical axis represents BrdU uptake and horizontal axis represents total DNA. The gates represent SubG1 (apoptotic cells), G1, S and G2/M phase from left to right, in this order. Numbers show the percentage of cells falling in each gate. Fig. S2 relates to Fig. 2.

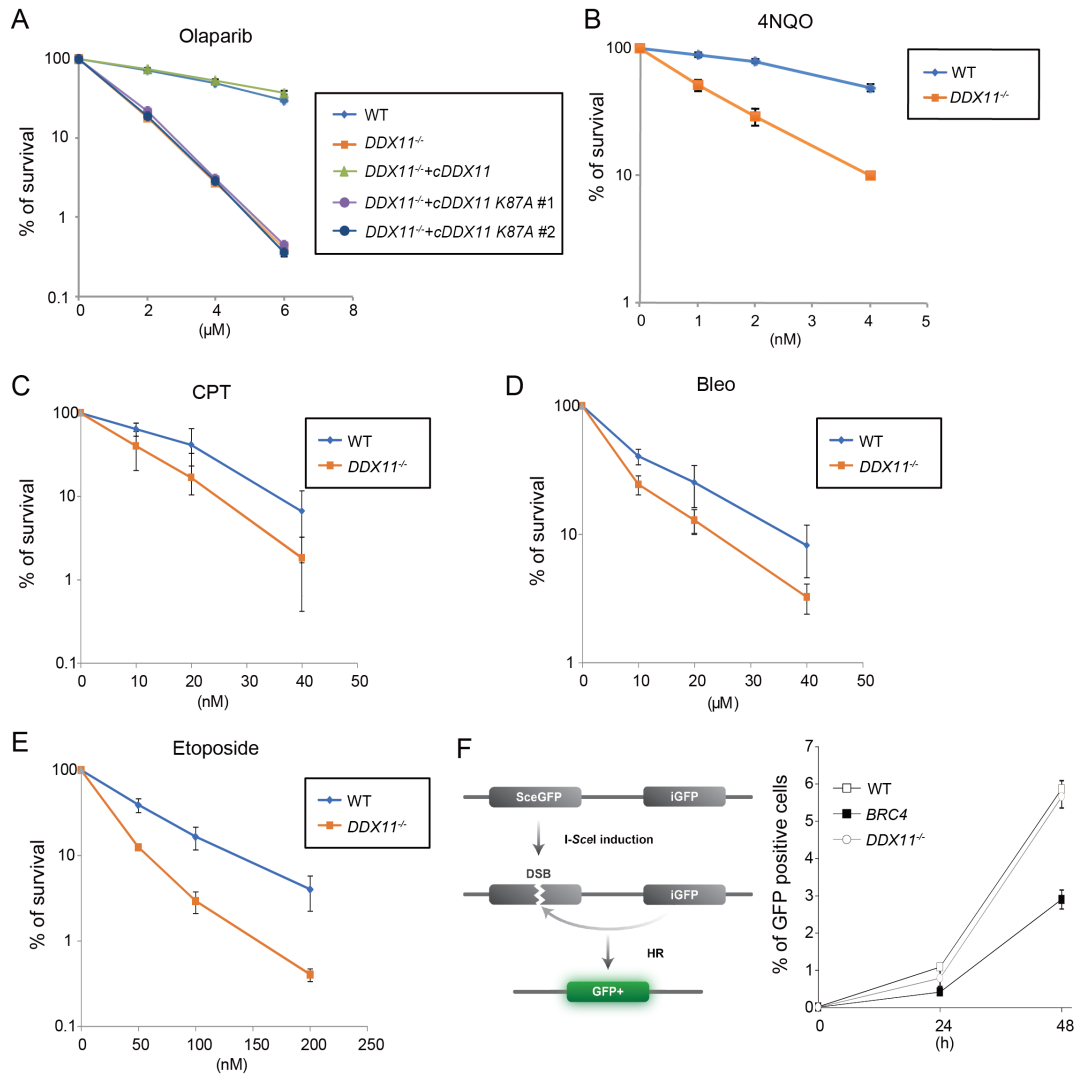


Figure S3. Drug sensitivity profile and proficiency in DSB repair in *ddx11* cells.

Sensitivity of WT and *ddx11* cells (A-E), complemented with DDX11 or DDX11 helicase-dead cDNA variants (A) to chronic treatments with the indicated drugs. CPT stands for camptothecin, Bleo for bleomycin. Cell survival was measured as in Fig. 1B. (F) The scheme of the GFP reporter-assay (left), and the rate of GFP positive cells (right). Fig. S3 relates to Fig. 3.

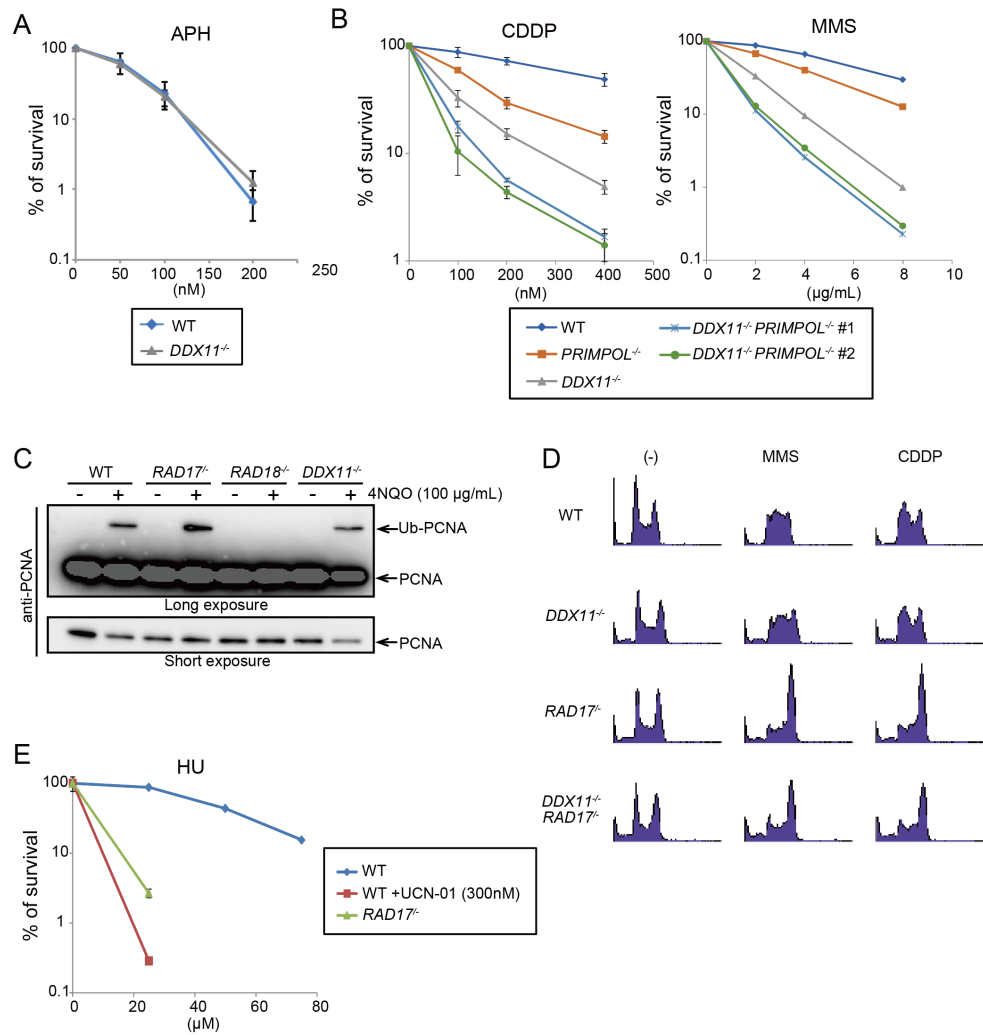


Figure S4. DDX11 is not required for the intra-S checkpoint, replication fork stability, PCNA ubiquitylation, and Primpol functions.

(A) Sensitivity of WT and *ddx11* cells to Aphidicolin (APH) as in Fig. 1B. (B) Sensitivity of cells of the indicated genotypes to CDDP and MMS. (C) RAD18-dependent PCNA ubiquitylation induced by 4NQO is proficient in *rad17* and *ddx11* cells. PCNA and its modifications were detected with the PC-10 antibody (sc-56). (D) Cell cycle analysis after MMS or CDDP exposure. Indicated cells were treated with 4×10^{-5} v/v MMS or $1 \mu\text{M}$ CDDP for 3 h or 6 h. Cells were fixed by 70% EtOH, stained with PI, and analyzed by FACS. (E) Cell survival of cells of the indicated genotypes to chronic HU treatment. Fig. S4 relates to Fig. 4.

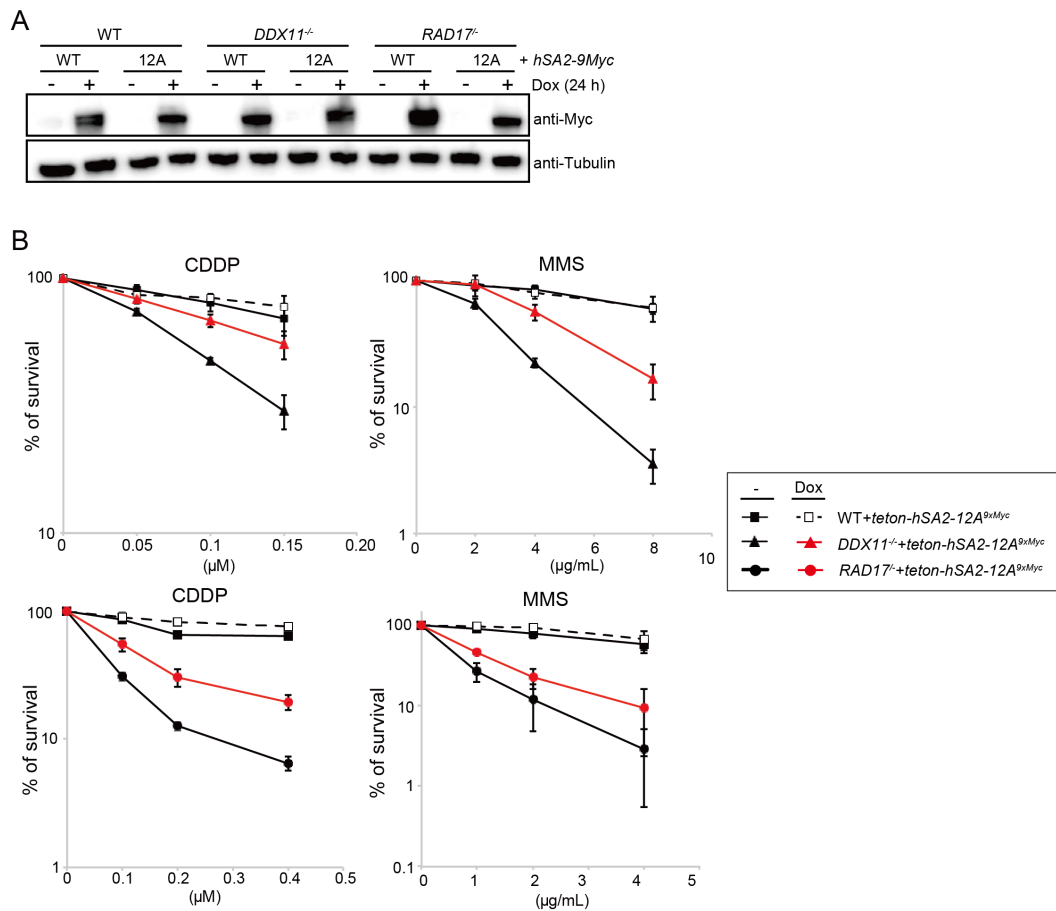


Figure S5. Lesions accumulating in *ddx11* and *rad17* cells can be repaired postreplicatively. (A) Expression levels of SA2 and SA2-12A in WT, *ddx11* and *rad17* cells. (B) Cellular sensitivity of WT, *ddx11* and *rad17* cells expressing or not Doxycycline-inducible SA2-12A to CDDP and MMS measured as in Fig. 1B. Figure S5 relates to Fig.4.

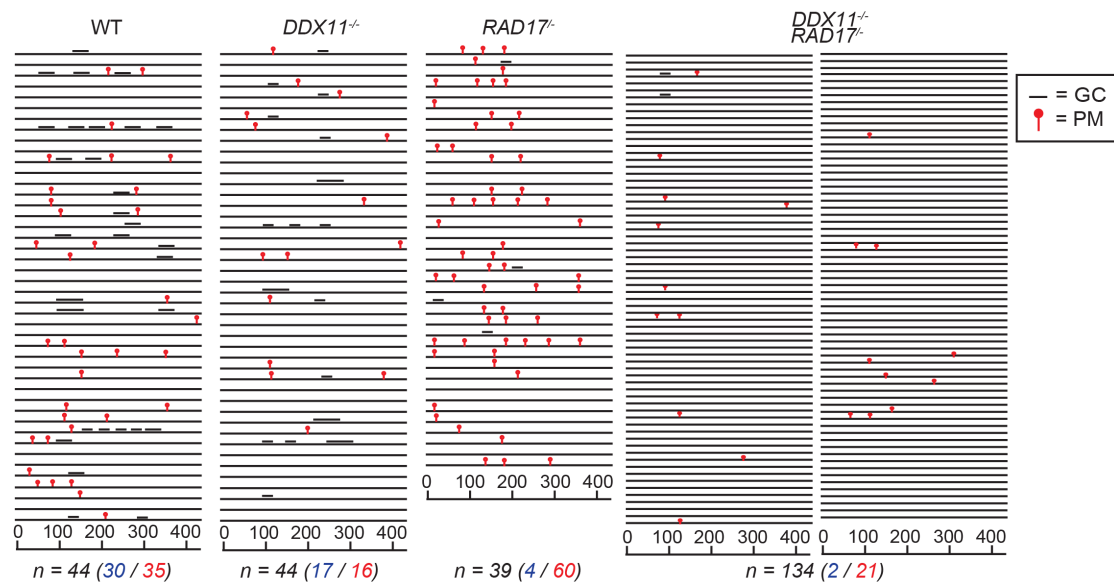


Figure S6. DDX11 facilitates replication through abasic sites and repair of bulky lesions.

Libraries of IgVλ segments isolated from the indicated mutants. Each mutant was cultured for 2 weeks under AID overexpressing conditions. Horizontal lines represent the rearranged IgVλ (410 bp), with hypermutation (red lollipop shapes) or gene conversion (horizontal bars). The number n indicates the number of sequenced individual IgVλ segments, in dark blue the number of gene conversion events, in red the number of point mutation events.